

Thermally Stable Self-Assembling Open-Frameworks: Isostructural Cs^+ and $(\text{CH}_3)_4\text{N}^+$ Iron Germanium Sulfides

Carol L. Bowes, Alan J. Lough, Andrzej Malek, Geoffrey A. Ozin*, Srebri Petrov, and David Young

Materials Chemistry Research Group, Lash Miller Chemical Laboratories, University of Toronto, 80 St. George Street, Toronto, Ontario, Canada M5S 1A1

Received December 18, 1995

Key Words: Self-assembling frameworks / Thermal stability

Here we report on investigations that have revealed for the first time that the Cs^+ ion templates the same metal germanium sulfide open-framework as $(\text{CH}_3)_4\text{N}^+$ (TMA^+), and that metal complexing agents enhance crystal size by at least two orders of magnitude. The synthesis, structures and thermal properties of $\text{Cs}_2\text{FeGe}_4\text{S}_{10} \cdot x \text{H}_2\text{O}$ and $\text{TMA}_2\text{FeGe}_4\text{S}_{10}$ are also described. Both have 3D zinc blende-type open-framework structures. These materials have the same connectivity as $\text{TMA}_2\text{MnGe}_4\text{S}_{10}$. The tetrahedral sites in the lattice are alternately substituted by pseudo-tetrahedral Fe^{2+} and adamantanoid $\text{Ge}_4\text{S}_{10}^{4-}$ building blocks, covalently linked together by $\text{Fe}(\mu\text{-S})\text{Ge}$ bridge bonds, to give a tetragonal unit cell. The charge-balance of the anionic framework $[\text{FeGe}_4\text{S}_{10}]^{2-}$ is maintained by either Cs^+ or TMA^+ ions in the cavity spaces. Synthesis of these materials demonstrates an

interesting example of a self-assembly process in which a 3D framework is built from molecular precursors. Water adsorption-desorption cycling from room temperature to 200°C reveals framework flexibility between larger and smaller tetragonal unit cell $\text{I}\bar{4}$ isotypes. The compound $\text{TMA}_2\text{FeGe}_4\text{S}_{10}$ is stable in nitrogen at 350°C and under vacuum at 450°C . The corresponding temperatures for $\text{Cs}_2\text{FeGe}_4\text{S}_{10}$ are 530°C and 630°C ; it is stable on cooling to room temperature under vacuum, and after subsequent exposure to air. Six hundred thirty degrees celsius is the highest recorded temperature at which the integrity of a non-oxide framework has been maintained. The framework stability and flexibility of "all-inorganic" $\text{Cs}_2\text{FeGe}_4\text{S}_{10}$ provides an encouraging example for researchers interested in developing sulfide-based framework materials with practical applications.

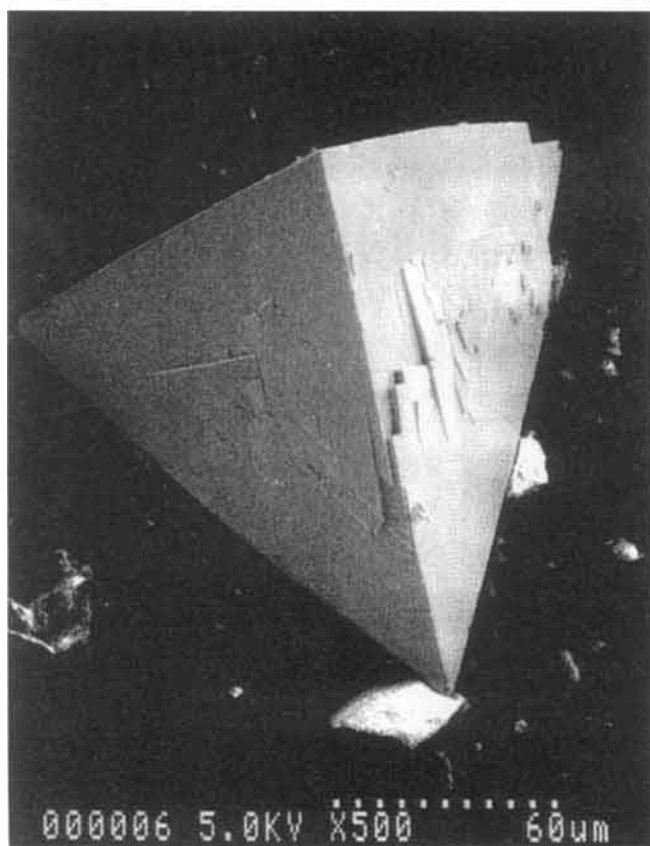
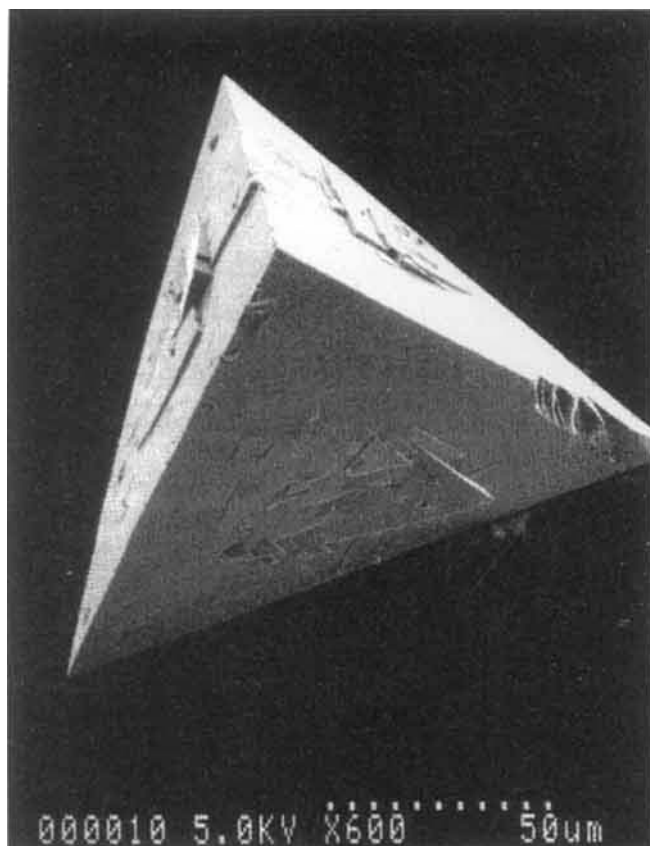
Aluminosilicate zeolites are typically crystallized with either alkali metal or organo cations present in their channels^[1,2]. Similarly, a cornucopia of non-oxide open-framework materials can be prepared with a variety of inorganic and organic structure-directing cations^[3–15]. One such example is the family of materials denoted TMA-MeGS-3, where Me is Mn, Fe, Co, or Zn, and TMA is tetramethylammonium^[5,8,9]. Bedard et al. was the first to report phases of this type in 1989^[5] and, recently, Yaghi et al. successfully solved the single crystal structure of TMA-MnGS-3 ($\text{TMA}_2\text{MnGe}_4\text{S}_{10}$) which was subsequently confirmed by ab initio structure determination methods by Achak et al. from pXRD data^[8]. We have been active in this field for several years, and recently published a number of papers which describe the crystal structures and physico-chemical properties of metal chalcogenide self-assembling frameworks and their potential for chemical sensing applications^[3,4,6,9–15]. The primary objective of this study was to determine whether Cs^+ can template the same metal germanium sulfide open-framework as $(\text{CH}_3)_4\text{N}^+$ (TMA^+). A secondary goal was the evaluation of the thermal properties of these materials.

The Cs^+ and $(\text{CH}_3)_4\text{N}^+$ (TMA^+) template mediated synthesis, single crystal XRD structure determination and thermal properties of $\text{Cs}_2\text{FeGe}_4\text{S}_{10} \cdot x \text{H}_2\text{O}$ and $\text{TMA}_2\text{FeGe}_4\text{S}_{10}$ are reported here for the first time. These materials have isostructural zinc blende-type iron, germanium, and sulfide open-frameworks; they exhibit impressive framework stability, and in the case of $\text{Cs}_2\text{FeGe}_4\text{S}_{10} \cdot x \text{H}_2\text{O}$, framework flexibility. In a procedure similar to that reported for $\text{TMA}_2\text{MnGe}_4\text{S}_{10}$, they were prepared by a two step reaction sequence^[8]. Elemental Ge (99.99%, Aldrich) and S (99.999%, Aldrich), in stoichiometric amounts, were hydrothermally digested in a 5% excess of aqueous TMAOH or CsOH ($\text{H}_2\text{O}/\text{Ge} = 50$; 150°C , tumbled, 16 hours). From the resultant solution, $\text{TMA}_4\text{Ge}_4\text{S}_{10}$ or $\text{Cs}_4\text{Ge}_4\text{S}_{10}$ was precipitated by adding acetone/ethanol. It was then

recovered by filtration or centrifugation, and purified and characterized (pXRD, Raman). Monoclinic salts of $\text{Cs}_4\text{Ge}_4\text{S}_{10} \cdot 3 \text{H}_2\text{O}$ and $\text{Cs}_4\text{Ge}_4\text{S}_{10} \cdot 4 \text{H}_2\text{O}$ were previously reported, along with their vibrational spectra^[16,17]. Yields of greater than 95% were readily achieved for the $\text{TMA}_4\text{Ge}_4\text{S}_{10}$ material with greater than 99.99% purity^[9]. Use of $\text{TMA}_4\text{Ge}_4\text{S}_{10}$ or $\text{Cs}_4\text{Ge}_4\text{S}_{10}$ as synthetic precursors avoided inhomogeneous and insoluble GeS_2 , which can often contain impurities deleterious to the crystallization of metal chalcogenide open frameworks. This tetrameric species is highly soluble in water. Addition of aqueous Fe^{2+} to $\text{Ge}_4\text{S}_{10}^{4-}$ solutions, in a molar ratio of 1:1, resulted in the crystallization of $\text{TMA}_2\text{FeGe}_4\text{S}_{10}$ and $\text{Cs}_2\text{FeGe}_4\text{S}_{10} \cdot x \text{H}_2\text{O}$, (elemental analysis, SEM-EDX). However, product crystals were typically 0.1 to 5.0 μm . By applying diffusion crystal growth techniques and/or selective complexing, mineralizing and transporting agents, we successfully grew high quality pseudo-tetrahedral single crystals of these materials as long as several hundred microns; see Figure 1^[9]. In the case of the $\text{FeGe}_4\text{S}_{10}$ phases, fluoride/hydroxide and triethanolamine complexed the Fe^{2+} ions. The stability of the resultant complexes controlled the release of metal species for reaction with aqueous $\text{Ge}_4\text{S}_{10}^{4-}$ moieties to form the open frameworks. The metal-to-complexing-agent ratio was one-to-one.

Low temperature single crystal X-ray diffraction structure evaluation showed that the materials are isostructural^[18,19]. CeriusTM, generated graphic representations of pertinent $[hkl]$ projections of these materials are shown in Figure 2. Both $\text{Cs}_2\text{FeGe}_4\text{S}_{10} \cdot x \text{H}_2\text{O}$ and $\text{TMA}_2\text{FeGe}_4\text{S}_{10}$ have 3D zinc blende-type open-framework structures with the tetragonal space group $\text{I}\bar{4}$; their unit cell dimensions are $a = 8.413(7) \text{ \AA}$, $c = 14.750(2) \text{ \AA}$ and $a = 9.374(3) \text{ \AA}$, $c = 14.174(4) \text{ \AA}$, respectively. Their overall architecture is most easily visualized in terms of the substitution of the tetrahedral sites in the zinc blende lattice, alternatively, by pseudo-tetrahedral Me^{2+} and

Figure 1. Scanning electron micrograph images of pseudotetrahedral morphology crystals of (top) $\text{Cs}_2\text{FeGe}_4\text{S}_{10} \cdot x\text{H}_2\text{O}$ and (bottom) $\text{TMA}_2\text{FeGe}_4\text{S}_{10}$



adamantanoid $\text{Ge}_4\text{S}_{10}^{4-}$ building blocks, all covalently linked together by $\text{Fe}(\mu\text{-S})\text{Ge}$ bridge bonds.

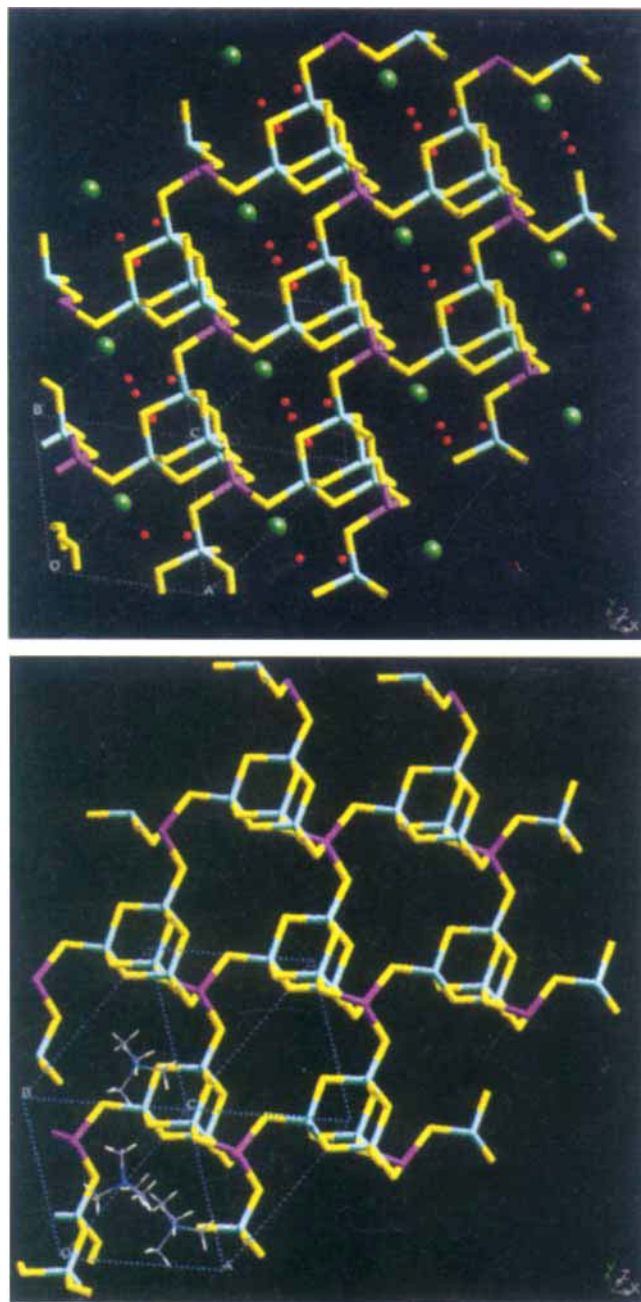
Charge-balance of the anionic framework $[\text{FeGe}_4\text{S}_{10}]^{2-}$ is maintained by either two Cs^+ or TMA^+ template ions. In the case of $\text{TMA}_2\text{FeGe}_4\text{S}_{10}$, both TMA^+ ions are located on 4 sites (4×0.25 occupancy) within the cavity spaces of the open-framework structure. The situation is different for $\text{Cs}_2\text{FeGe}_4\text{S}_{10} \cdot x\text{H}_2\text{O}$. One Cs^+ was found and is statically disordered over $\bar{4}$ (4×0.225) and 1 (1×0.230) sites. The other remains unlocated in the cavity spaces due to hydration and dynamical disorder. This second Cs^+ was detected by bulk chemical analysis, which gave the formula of this phase as $\text{Cs}_{1.86}\text{Fe}_{1.08}\text{Ge}_{4.00}\text{S}_{9.88}$. Two crystallographically distinct kinds of H_2O molecules with a total occupancy of 0.5 are contained in $\text{Cs}_2\text{FeGe}_4\text{S}_{10} \cdot x\text{H}_2\text{O}$. These are best ascribed to framework, hydrogen bonded forms of H_2O . The unlocated H_2O is likely the physisorbed form (see TGA/PXRD below).

The Fe^{2+} connector in $\text{Cs}_2\text{FeGe}_4\text{S}_{10} \cdot x\text{H}_2\text{O}$ and $\text{TMA}_2\text{FeGe}_4\text{S}_{10}$ has a squashed tetrahedral coordination geometry with essentially the same Fe-S bond lengths of 2.325(11) Å and 2.348(7) Å. The respective S-Fe-S bond angles are 116° , 106.3° and 122.4° , 103.4° . This change in the S-Fe-S bond angles results in a net contraction in the unit cell from 1245.5(7) Å³ for $\text{TMA}_2\text{FeGe}_4\text{S}_{10}$ to 1044.0(2) Å³ for $\text{Cs}_2\text{FeGe}_4\text{S}_{10} \cdot x\text{H}_2\text{O}$. The higher ionic potential (effective charge-to-radius ratio) of Cs^+ as compared to TMA^+ results in shorter cesium-sulfur contact interactions with nearest neighbor framework sulfur atoms of the $\text{Ge}_4\text{S}_{10}^{4-}$ adamantanoid units. This appears to be responsible for the observed lengthening and shortening, respectively, of the tetragonal c and a unit cell parameters in $\text{Cs}_2\text{FeGe}_4\text{S}_{10} \cdot x\text{H}_2\text{O}$ as compared to $\text{TMA}_2\text{FeGe}_4\text{S}_{10}$. This property changes the effective dimensions of the channels (size and shape); see Figure 2. It bodes well for the use of these kinds of nanoporous metal sulfides in materials requiring tunable pore sizes such as sulfur tolerant catalysts, molecular sieves or chemoselective sensors.

The thermochemical properties of $\text{Cs}_2\text{FeGe}_4\text{S}_{10} \cdot x\text{H}_2\text{O}$ and $\text{TMA}_2\text{FeGe}_4\text{S}_{10}$ were investigated by TGA-MS and variable temperature in situ PXRD. The TGA of "all-inorganic" $\text{Cs}_2\text{FeGe}_4\text{S}_{10} \cdot x\text{H}_2\text{O}$ under N_2 showed thermal transitions around 116°C (4.6 wt.%) and 188°C (4.1 wt.%), followed by a series of sharp thermal transitions commencing around 510°C and continuing beyond 700°C (8.9 wt.%); see Figure 3. The first two weight losses correspond to roughly 2.4 H_2O and 0.3 H_2O molecules per $\text{Cs}_2\text{FeGe}_4\text{S}_{10}$ formula unit. They are associated with the physisorbed and framework, hydrogen bonded (chemisorbed) forms of H_2O ; the latter was located in the single crystal XRD structure analysis. In an analogy to zeolites, the water content, $x\text{H}_2\text{O}$, appears to be humidity dependent. Support for this proposal stems from the indexing of in situ PXRD data. Physisorbed/chemisorbed water adsorption-desorption cycling revealed framework flexibility between tetragonal $\bar{14}$ [$a = 8.414(7)$ Å, $c = 14.753(2)$ Å] and a smaller tetragonal $\bar{14}$ [$a = 8.253(2)$ Å, $c = 14.784(5)$ Å] isotype; see Figure 4 ($\Delta V = -37.47$ Å³, -3.6%). In view of the sublimation temperatures reported for GeS (450°C) and GeS_2 (600°C), it is possible that the higher temperature thermal transitions associated with the collapse of the framework involve redox processes and sublimation losses of these materials from dehydrated $\text{Cs}_2\text{FeGe}_4\text{S}_{10}$; see Figure 5. The solid products of this reaction were found to be PXRD amorphous.

The first TGA thermal event of $\text{TMA}_2\text{FeGe}_4\text{S}_{10}$ under nitrogen occurred around 315°C (note that there was no sign of water in this material) and corresponded to a weight loss of 27.5 wt.%; see Figure 3. This weight loss was twice that observed by Yaghi et al. for $\text{TMA}_2\text{MnGe}_4\text{S}_{10}$ ^[8]. This was followed by a smooth weight loss

Figure 2. Framework projections of the single crystal XRD structures of (top) $\text{Cs}_2\text{FeGe}_4\text{S}_{10} \cdot x\text{H}_2\text{O}$ and (bottom) $\text{TMA}_2\text{FeGe}_4\text{S}_{10}$. These representations show a 3D zinc blende lattice of $\text{Fe}(\mu\text{-S})\text{Ge}$ covalently bridged pseudo-tetrahedral Fe^{2+} and adamantanoid $\text{Ge}_4\text{S}_{10}^{4-}$ building blocks. (green = Cs, pink = Fe, light blue = Ge, yellow = S, red = O, dark blue = N, grey = C, white = H)



continuing beyond 700 °C and amounting to 6.3 wt.%. Mass spectroscopic examination of the evolved volatilized species at the 315 °C event combined with the TGA data defines the process as template-loss and framework decomposition with the reaction stoichiometry:



The solid product(s) of this reaction were also found to be PXRD amorphous. This high temperature aspect of the study needs further work to better define the thermochemical properties of the materials.

Figure 3. TGA-DTGA traces for (bottom) $\text{Cs}_2\text{FeGe}_4\text{S}_{10} \cdot x\text{H}_2\text{O}$ and (top) $\text{TMA}_2\text{FeGe}_4\text{S}_{10}$ recorded under nitrogen

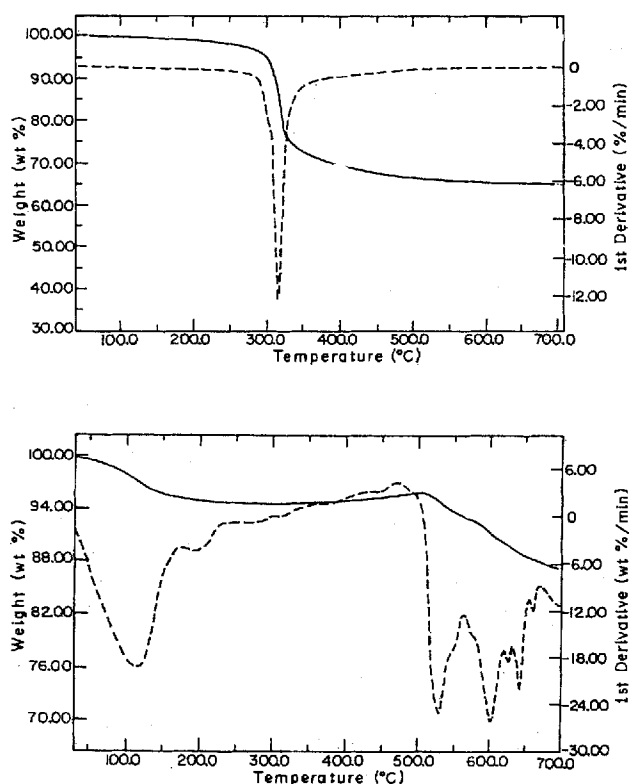
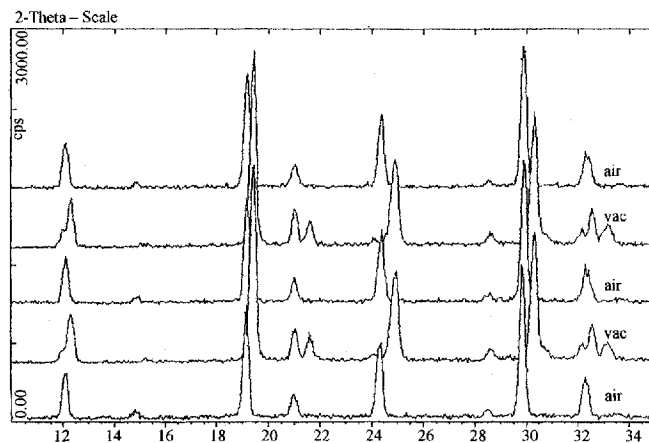


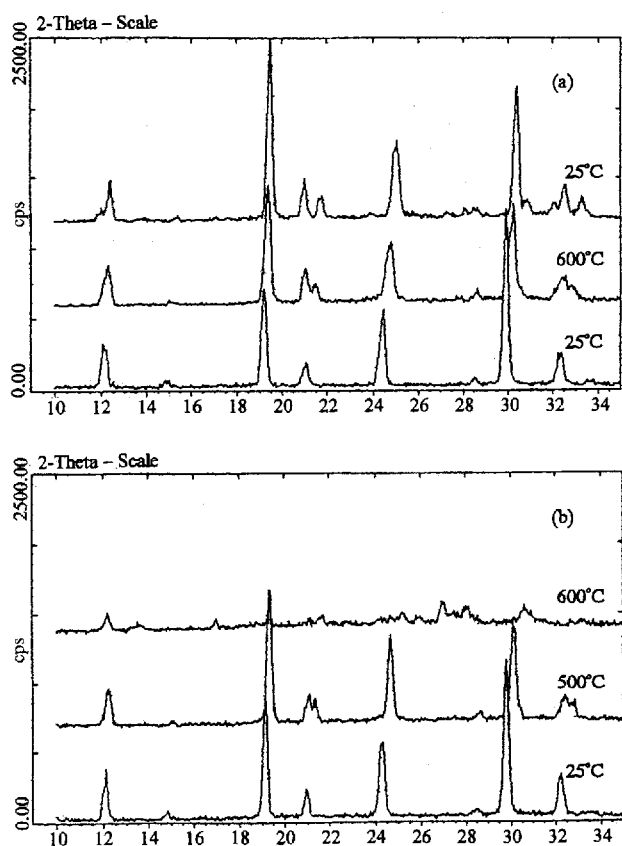
Figure 4. Water adsorption-desorption cycling effects on in situ PXRD traces for $\text{Cs}_2\text{FeGe}_4\text{S}_{10} \cdot x\text{H}_2\text{O}$



The corresponding variable-temperature in situ PXRD data for $\text{TMA}_2\text{FeGe}_4\text{S}_{10}$ under nitrogen and dynamic vacuum are shown in Figure 6. In the case of $\text{TMA}_2\text{FeGe}_4\text{S}_{10}$ under nitrogen, the loss of the TMA^+ template around 350 °C was accompanied by irreversible collapse of the open-framework structure, Figure 6(b). In vacuum, it showed little sign of collapse up until 400 °C, Figure 6(a).

Under nitrogen, deleterious attack of the framework by reactive organic template fragments caused breakdown of the entire structure, whereas these effects were minimized under vacuum. $\text{TMA}_2\text{FeGe}_4\text{S}_{10}$ under vacuum at 425 °C had PXRD crystallinity comparable to the material at room temperature. Moreover, it was

Figure 5. Variable temperature, in situ PXRD data for $\text{Cs}_2\text{FeGe}_4\text{S}_{10} \cdot x\text{H}_2\text{O}$ recorded under (a) dynamic vacuum and (b) in nitrogen



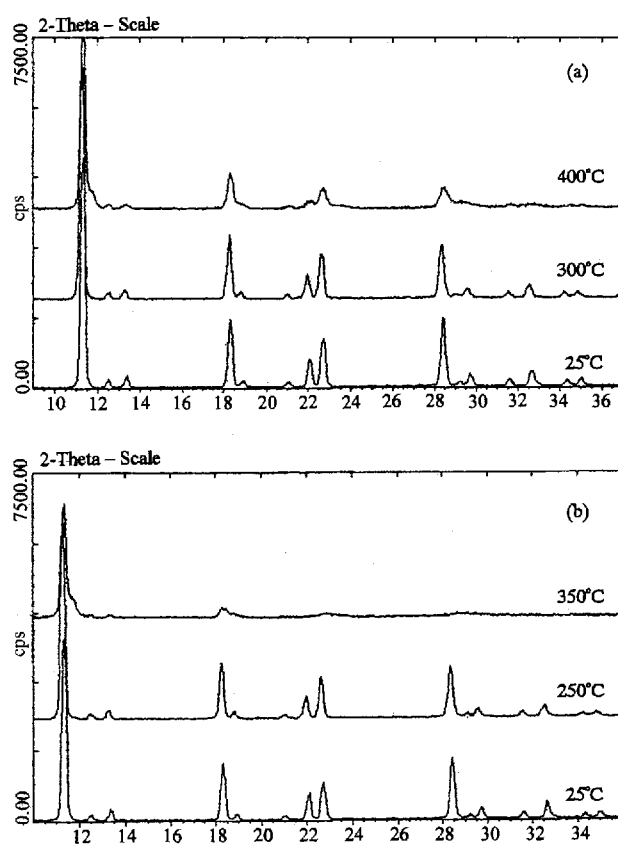
stable on cooling to room temperature in vacuum and after subsequent exposure to air.

Under nitrogen at around 100–200°C, the isotype $\text{Cs}_2\text{FeGe}_4\text{S}_{10} \cdot x\text{H}_2\text{O}$ dehydrated and underwent what is best described as a shrinkage of the unit cell, with maintenance of the tetragonal $I\bar{4}$ symmetry, Figure 5(b). This phenomenon is associated with the desorption of the physisorbed and chemisorbed H_2O molecules from the structure. The process was reversed on reexposure to H_2O . Water adsorption-desorption cycling between the tetragonal $I\bar{4}$ $\text{Cs}_2\text{FeGe}_4\text{S}_{10} \cdot x\text{H}_2\text{O}$ and smaller unit cell dehydrated $\text{Cs}_2\text{FeGe}_4\text{S}_{10}$ isotype, revealed the flexibility of this framework, see Figure 4. Significantly, under vacuum the integrity of the framework was maintained intact until at least 600°C, Figure 5(a). There was no detectable difference in the degree of crystallinity of the material at the extremes of room temperature and high temperature. This is by far the highest recorded temperature at which the integrity of a “nonoxide based open-framework material” is maintained.

Ongoing investigations of these kinds of nanoporous metal germanium sulfide clusters will focus attention on compositional tuning of their electronic and optical properties, single crystal growth and their potential for molecule-discriminating chemical sensing.

The generous financial assistance of the *Natural Sciences and Engineering Research Council of Canada* (NSERC), the *Canadian Space Agency* (CSA), and *Universal Oil Products* (UOP) is deeply appreciated. The technical assistance of Ms. *Wendy Huynh* is highly valued. The SEM/EDX data were supplied by Dr. *Neil Coombs* (Imagetek) and the elemental analyses were performed by Dr. *Walter Zamachek* (UOP). Stimulating and informative discussions with Mr. *Scott Kirkby* are gratefully acknowledged.

Figure 6. Variable temperature in situ PXRD data for $\text{TMA}_2\text{FeGe}_4\text{S}_{10}$ recorded under (a) dynamic vacuum and (b) in nitrogen



Experimental

Crystal Data for $[\text{FeGe}_4\text{S}_{10} \cdot 2(\text{Me}_4\text{N})]$, $\text{C}_8\text{H}_{24}\text{FeGe}_4\text{N}_2\text{S}_{10}$: $M_r = 815.12$, tetragonal, space group $I\bar{4}$ (no. 82), $a = 9.374(3)$, $c = 14.174(4)$ Å, $V = 1245.5(7)$ Å³, $D_c = 2.173$ g cm^{−3}, $Z = 2$, Mo- $K\alpha$ radiation, $\lambda = 0.71073$ Å, $\mu(\text{Mo}-K\alpha) = 6.178$ mm^{−1}, $T = 173(2)$ K. Siemens P4 diffractometer, 881 reflections collected $6 < 2\theta < 50^\circ$, semi-empirical absorption correction^[18] (minimum and maximum transmission factors 0.2458 and 0.6380), 803 unique ($R_{\text{int}} = 0.122$), structure solved by direct methods and refined by full-matrix least-squares based on F^2 ^[19]. All non-hydrogen atoms refined with anisotropic displacement parameters. H atoms were included in calculated positions ($\text{C}-\text{H} = 0.96$). $R1 = 0.678$, $wR2 = 0.0961$ for 492 reflections with $F > 4\sigma(F)$ and $R1 = 0.1478$, $wR2 = 0.1231$ (all data). Minimum and maximum peaks in the final ΔF map -0.909 and 1.090 eÅ^{−3}.

Crystal Data for $[\text{FeGe}_4\text{S}_{10} \cdot \text{Cs}_2(\text{H}_2\text{O})_{0.42}]$: $M_r = 940.2$, tetragonal, space group $I\bar{4}$ (no. 82), $a = 8.413(7)$, $c = 14.75(2)$ Å, $V = 1044(2)$ Å³, $D_c = 2.99$ g cm^{−3}, $Z = 2$, Mo- $K\alpha$ radiation, $\lambda = 0.71073$ Å, $\mu(\text{Mo}-K\alpha) = 10.78$ mm^{−1}, $T = 173(2)$ K. Siemens P4 diffractometer, 410 reflections collected $7 < 2\theta < 54^\circ$, semi-empirical absorption correction^[18] (minimum and maximum absorption corrections were 0.1538 and 0.3681), 406 unique reflections ($R_{\text{int}} = 0.082$), structure solved by direct methods and refined by full-matrix least-squares based on F^2 ^[19]. $R1 = 0.0606$, $wR2 = 0.1105$ for 272 reflections with $F > 4\sigma(F)$ and $R1 = 0.1075$, $wR2 = 0.1399$ for all data, minimum and maximum features in the final difference map were 0.709 and -0.912 eÅ^{−3}. The empirical formula calculated from elemental analysis is $\text{FeGe}_4\text{S}_{10} \cdot \text{Cs}_2(\text{H}_2\text{O})_x$.

Only 1.27 Cs atoms were located in the X-ray structure. It is presumed that the remaining contribution is disordered over many sites (in a fashion analogous to the extra-framework cations in zeolites^[1]) and is therefore not visible in a difference Fourier map. An electron density peak, of approximately $4 \text{ e}\text{\AA}^{-3}$, located in the penultimate difference Fourier map, was refined as a partial oxygen (H_2O) site.

Further details of the crystal structure investigation are available on request from the Director of the Cambridge Crystallographic Data Centre, 12 Union Road, GB-Cambridge CB12 1EZ (UK), on quoting the full journal citation.

- [1] D. W. Breck, *Zeolite Molecular Sieves*, John Wiley and Sons, New York, 1974.
- [2] R. M. Barrer, *Hydrothermal Chemistry of Zeolites*, Academic Press, London, 1982.
- [3] G. A. Ozin, *Adv. Mater.* **1992**, *4*, 612; G. A. Ozin in *Materials Chemistry: An Emerging Subdiscipline* (A.C.S. Symposium, Washington, March 1992), *A.C.S. Symp. Ser.*, (Ed.: L. Interrante), Washington, 1994; G. A. Ozin, C. L. Bowes, *Mater. Res. Soc. Symp. Proc.* **1992**, *286*, 93.
- [4] G. A. Ozin, "Microporous and Mesoporous Electronic Materials: Open-Framework Nanomaterials for Molecular Recognition, Towards the Electronic Nose", *Supramolecular Chemistry*, in press.
- [5] R. L. Bedard, L. D. Vail, S. T. Wilson, E. M. Flanigen (UOP), U.S. Pat. Patent 4,880,761, 1989; R. L. Bedard, L. D. Vail, S. T. Wilson, E. M. Flanigen (UOP), U.S. Patent 4,933,068, 1990;
- R. I. Bedard, S. T. Wilson, L. D. Vail, J. M. Bennett, E. M. Flanigen in *Zeolites: Facts, Figures and Future* (Eds.: P. A. Jacobs, R. A. van Santen) Elsevier, Amsterdam, 1989.
- [6] T. Jiang, A. J. Lough, G. A. Ozin, D. Young, *Chem. Mater.* **1995**, *7*, 245.
- [7] Y. Ko, K. Tan, D. M. Nellis, S. Koch, J. B. Parise, *J. Solid State Chem.* **1995**, *114*, 506.
- [8] O. M. Yaghi, Z. Sun, D. A. Richardson, T. L. Groy, *J. Am. Chem. Soc.* **1994**, *116*, 807; O. M. Yaghi, D. A. Richardson, G. Li, C. E. Davis, T. L. Groy, *Mat. Res. Soc. Symp. Proc.*, **1995**, *371*, 15; O. Achak, J. Y. Pivan, M. Maunaye, M. Louër, D. Louër, *J. Alloys Comp.*, **1995**, *219*, 111.
- [9] S. J. Kirkby, PhD Thesis (Spectroscopy of Metal Germanium Chalcogenide Framework Materials and Precursors), Univ. of Toronto, 1996; and unpublished results.
- [10] T. Jiang, G. A. Ozin, R. L. Bedard, *Adv. Mater.* **1994**, *6*, 860.
- [11] R. L. Bedard, P. Enzel, G. S. Henderson, G. A. Ozin, *Adv. Mater.* **1995**, *7*, 64.
- [12] T. Jiang, G. A. Ozin, R. L. Bedard, *Adv. Mater.* **1995**, *7*, 166.
- [13] H. Ahari, R. L. Bedard, C. L. Bowes, T. Jiang, A. J. Lough, G. A. Ozin, S. Petrov, D. Young, *Adv. Mater.* **1995**, *7*, 375.
- [14] H. Ahari, R. L. Bedard, A. J. Lough, S. Petrov, G. A. Ozin, D. Young, *Adv. Mater.* **1995**, *7*, 370.
- [15] H. Ahari, R. L. Bedard, C. L. Bowes, T. Jiang, S. J. Kirkby, A. Kuperman, A. J. Lough, G. A. Ozin, S. Petrov, A. Verma, D. Young, *Adv. Mater.*, in press.
- [16] V. S. Pohl, B. Krebs, *Z. Anorg. Allg. Chem.* **1976**, *424*, 265.
- [17] B. Krebs, S. Pohl, *Z. Naturforsch.* **1971**, *26b*, 853.
- [18] Sheldrick, G. M., SHELXA-90, Program for Absorption Correction, University of Göttingen, Germany.
- [19] Sheldrick, G. M., SHELXLTL/PC V5.0, Siemens Analytical X-ray Instruments, Madison, Wisconsin, USA.

[95207]